Static and Time-Dependent Analyses of Tidally Induced Faulting within Europa's Ice Shell: Implications for Subsurface Communication Development.

Rudi R. Lien[1,2], Kathleen L. Craft[2], Matthew E. Walker[3], G. Wesley Patterson[2], and Alyssa R. Rhoden[4]. [1]University of Oregon, Eugene, OR (rlien@uoregon.edu), [2]Johns Hopkins University Applied Physics Laboratory, Laurel, MD, [3]Planetary Science Institute, [4]Southwest Research Institute, Boulder, CO.

Introduction: Europa, a satellite of Jupiter in the outer solar system, potentially hosts the necessary conditions to support life. Although Europa receives minimal solar energy and heat due to its distance from the Sun, evidence suggests that large gravitational forcing from Jupiter produces enough internal heat to sustain a liquid water ocean underneath an ice shell [1-2]. A future subsurface mission to explore the ocean at Europa would need to be capable of descending up to 10s of km through the ice shell while maintaining communications back to Earth throughout the duration of the mission [3-4].

Europa's surface is abundant in fracture and fault-like structures, along which fault motion can initiate and potentially accumulate net offsets due to diurnal tidal stressing [5]. This tidally induced fault motion could pose a threat to a subsurface probe (i.e. cryobot) and its communication hardware, likely an optical tether extending from the surface and/or free space repeaters. To assess the potential hazards associated with a subsurface mission, we used the Ansys Mechanical numerical modeling software to determine the potential magnitude of tidally induced fault motion and associated strain (assuming no tether slip, i.e. tether moves with the fault) on a communication tether under static and time-dependent stress conditions, for all combinations of parameters in Table 1.

Table 1. Parameters for 3D Fault Models.

Parameter	Static	Time-dependent
Fault angle, θ (from vertical)	5-, 20-, 45- degrees	5-, 45-degrees
Fault Orientation	East-dipping, North-dipping	North-dipping
Geographic Location	Subjovian (0°, 0°), Thera Macula (50°S, 180°E)	Thera Macula (50°S, 180°E)
Coefficient of Friction, μ	0.1 or 0.55	0.1
True anomaly, f (relative to apojove)	180° (perijove)	0°-360°, every 30°
Number of Models	18	2

Methods: In this work, we considered the axisymmetric tidal potential that Europa is subjected to, due to its eccentric orbit, and determined the deformational response at the Subjovian (0°, 0°) and Thera Macula chaos terrain (50°S, 180°E) locations, at multiple true anomaly, *f*, positions, using methods that closely mirror *ref.* [6]. Results included the displacement, strain, and stress at 100 m resolution throughout the model domain.

Model set-up. A 3-dimensional block geometry represented a 3-km-long by 2-km-wide by 2.5-km-deep section of Europa's ice shell (Figure 1). We assumed a 10-km elastic shell of pure water ice, and material properties were homogeneous throughout the ice block (density = 920 kg/m^3; Poisson's ratio = 0.30; shear modulus = 3.5 GPa). All faces aside from the top and base of the ice block are fixed so that the block can only deform in the vertical direction at its boundaries, which represented the continuation of the ice shell beyond the modeled block. The base of the block was fixed with tidal displacements either computed at the Subjovian or Thera Macula chaos terrain for the corresponding true anomaly point. The top face represented the surface of Europa and was free to deform in all directions (free surface).

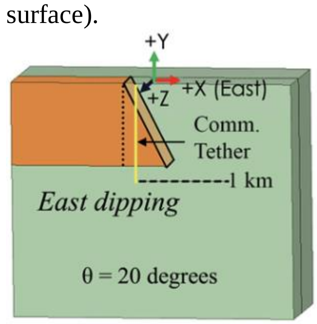

Figure 1. 3D fault model set-up. Figure is a cross-section at Z=0 (half of full block) to show fault plane in center.

A fault plane extending from the surface to 900-m depth and 500-m wide was added to the block at 5-, 20- and 45-degrees from vertical, either north- or east-dipping, and with a minimum or maximum coefficient of friction μ for water ice (Table 1). The contact between the hanging wall and footwall faces of the fault plane was set as a "frictional contact," allowing slip to occur along the plane when an equivalent shear stress, τ, was reached or exceeded: $\tau \geq \mu\sigma_n$, where σ_n is the normal stress acting on the fault plane. After each model run, directional displacements (X_{disp}, Y_{disp}, Z_{disp}) between the hanging wall and footwall were computed at multiple coordinates along the fault plane. From these outputs, the net fault displacement (displacement vector magnitude) was calculated and direction of fault motion was determined.

Static method. In previous work, static load models were set up to quantify net fault displacements and direction of motion due to maximum tidal bulging, at the perijove position of Europa's orbit (f = 180°) [7]. Tidal stress and displacements were computed at perijove for the Subjovian and Thera Macula regions and imported into each of the Ansys 3D fault models (Table 1). Results showed net fault displacements were <5 cm at the Subjovian and ~5-80 cm at Thera Macula, depending on fault angle and orientation, depth along the fault, and coefficient of friction [7], however potential buildup of stress and motion between apojove and perijove positions were not considered in the static analyses.

Time-dependent method. Two time-dependent models were set up to consider the accumulation of stress along the fault plane throughout Europa's orbit, due to changes in the imposed tidal stress and resultant fault displacements (model parameters shown in Table 1). We simulated fault motion at twelve time points (30-degree increments of true anomaly, f, relative to apojove) during one tidal cycle. For the initial model at t=0 (apojove position), tidal stress (computed for apojove, f=0°) was applied to the initially undeformed ice block. After t=0, the deformation of the ice block, including motion along the fault, was accounted for by transferring the deformed geometry and stress accumulation + change in tidal stress from one time point to the next. Net fault displacements were calculated at each time point.

Results: Time-dependent tidal forcing over one tidal cycle resulted in net fault displacements of ~0.50-2.9 m for end-member fault geometries at Thera Macula (Figure 2). Time-dependent results at perijove (t=6) were compared to the corresponding static model results to identify differences in results (if any) between the two methods. This comparison suggested that static models may provide accurate slip magnitude predictions for near-vertical fracture angles, but results differed significantly for the 45-degree fracture angle (Figure 2), indicating that the time-dependent method should be used for future adaptations of the model to best assess hazards at potential landing sites for future missions. Net offsets observed between the final (t=12) and initial positions (t=0) of the fault contact faces for both time-dependent models indicated that the fault did not return to its initial position, which potentially represents accumulated strain on a communication tether crossing the fault that is not relaxed after each tidal cycle.

Communication tether strain. To assess the potential risk to a subsurface mission by fault motion, we estimated the strain imposed on a communication tether crossing a fault. We assumed the change in tether length would be equal to the computed net fault displacement. Strain also depends on the length of the tether that is stretched, L_0. Here, tether strain was computed for potential L_0 end-members: 1) a small length of the tether in the region immediately near the fault (L_0 = 5.78 cm) or 2) the whole length of the tether (L_0 = 1 km), which assumes a cryobot at a depth of 1 km. The results for L_0 = 1 km did not exceed a strain of 10^{-3} (0.1%), while results for L_0 = 5.78 cm exceeded a strain of ≥60% in all models. Depending on L_0 and model parameters (Table 1), tether strain results ranged from 10^{-6} – 49.7 (Figure 2).

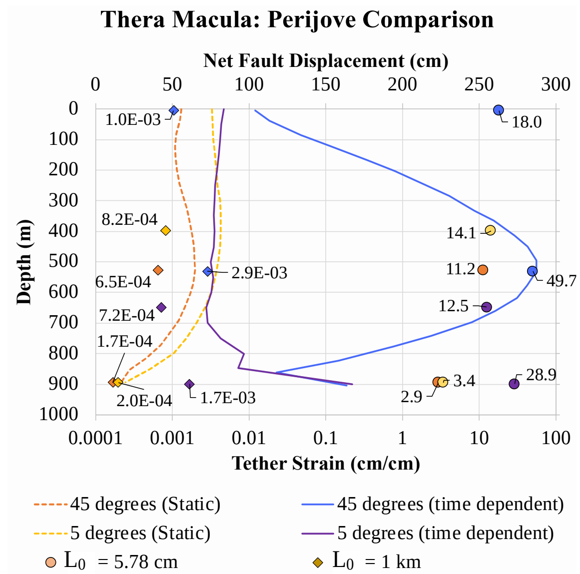

Figure 2. Net fault displacement and tether strain for static and time-dependent models at perijove with μ=0.1 for a 5- or 45-degree north-dipping fault at Thera Macula.

Constraints from Europa Clipper: The upcoming Europa Clipper mission may provide additional constraints on the models presented in this work [8]. As more ice shell data and imagery are collected, these fault models can be updated and used to assess the potential hazards at future exploration sites to determine those with survivable conditions for cryobot hardware.

Acknowledgments: This work is supported by funding from NASA SESAME grant 80NSSC19K0613.

References: [1] Ojakangas and Stevenson (1989) *Icarus*, *81*, 220-241. [2] Hussmann et al. (2002) *Icarus*, *156*, 143-151. [3] Oleson et al. (2019) Europa Tunnelbot, *NASA/TP*—2019-220054. [4] Craft et al. (2023) *54th LPSC*, Abs. #2252 [5] Sarid et al. (2002) *Icarus*, *158*, 24-41. [6] Walker and Rhoden (2022) *PSJ*, *3*, 149. [7] Lien et al. (2021) *GSA*, Abs. 43-8. [8] Pappalardo et al. (2021) *BAAS*, *53*, p. 255.